Available online at www.sciencedirect.com

ScienceDirect

Procedia Engineering 86 (2014) 215 – 222

Procedia Engineering

www.elsevier.com/locate/procedia

1st International Conference on Structural Integrity, ICONS-2014

Integrity Assessment of Grade 92 Welded Joint under Creep Condition

T. Sakthivel[a,*], K. Laha[a], K.S. Chandravathi[a], P. Parameswaran[a], H.M. Tailor[b], M. Vasudevan[a] and M.D. Mathew[a]

Metallurgy and Materials Group,
[a]*Indira Gandhi Centre for Atomic Research, Kalpakkam – 603102, India*
[b]*Institute for Plasma Research, Bhat, Gandhinagar, Gujarat – 382428, India*
[*]*E-mail ID: tsakthivel@igcar.gov.in*

Abstract

Integrity of tempered martensitic grade 92 (9Cr-1.8W-0.5Mo-VNb) steel welded joint has been assessed by carrying out creep test at 923 K over a wide stress range. The failure location in the joint was found to shift from base metal to heat affected zone (HAZ) of the weld joint with decrease in applied stress. The HAZ of the weld joint consisted of coarse prior-austenite grain (CGHAZ), fine prior-austenite grain (FGHAZ) and intercritical (ICHAZ) regions in a sequence from the fusion boundary to unaffected base metal. The failure was associated with localized creep deformation coupled with creep cavitation. To have a better insight to the creep failure behaviour of the joint, the different microstructural constituents of HAZ of the joint has been simulated. Creep and tensile tests were carried out on the simulated HAZs specimens. The steel suffered degradation in creep rupture strength on subjecting heating in the intercritical (between Ac_1 and Ac_3) (ICHAZ) as well as at temperature just above the Ac_3 (FCHAZ). The extensive creep cavitation has been observed in the simulated FGHAZ of the joint. Similarly, localized extensive creep cavitation and precipitation of tungsten rich Laves phase has been observed in the FGHAZ of the weld joint. This caused the type IV failure in the FGHAZ of the weld joint. The integrity of grade 92 steel joint under creep condition is governed by the above microstructural modifications of the steel in HAZ by weld thermal cycle.

Peer-review under responsibility of the Indira Gandhi Centre for Atomic Research

Keywords: ASME grade 92 ferritic steel, HAZs, Weld joint, Creep, Type IV cracking

1. Introduction

Martensitic 9 to 12 % chromium steels have widely been used in the fossil-fired and steam generators of nuclear power plants due to its excellent mechanical properties at high temperatures, good weldability, and adequate corrosion and stress-corrosion cracking resistances [1-13]. The increases in environmental concern and efficiency

Peer-review under responsibility of the Indira Gandhi Centre for Atomic Research
doi:10.1016/j.proeng.2014.11.031

have been the more concern lead to the development of new steels with improved properties for high temperatures applications. The addition of 1.8-2.0 wt.% tungsten and 0.002-0.005 wt.% boron with reduction of molybdenum to around 0.5 wt.% in grade 91 steel leads to the development of grade 92 steel. The steel derives its high temperature strength from tempered martensite lath structure, $M_{23}C_6$ type of carbide, intra-lath MX type carbide and nitride, transformation induced high dislocation density and solid solution strengthening from tungsten [4-7,13]. The mechanical properties of ASME grade 92 steel have been widely studied and the steel is used for high temperature components in fossil fired power plants [14-15]. Such large plants components are usually fabricated employing fusion welding as a joining process. It has been found that the creep rupture strength of weld joint of the steel as in other Cr-Mo-W ferritic steels is a life limiting factor. A premature creep failure occurs in and around the weld joint under operating condition. Fusion welded joint of 9Cr-ferritic steels consists of three different zones such as base metal, weld metal (fusion zone) and heat affected zone (HAZ). The HAZ is a transition region between weld metal and unaffected base metal, which can be subdivided into a number of zones depending upon the peak thermal cycles experienced during welding [10-14]. The HAZ consists of various microstructural constituents across it, such as coarse prior-austenite grain (CGHAZ) adjacent to the weld metal, fine prior-austenite grain (FGHAZ) adjacent to CGHAZ, and intercritical (ICHAZ) region, which is heated at temperature between Ac_1 and Ac_3, merging with the unaffected base metal [10-14]. Components associated with weld joints exposed in the service conditions at high temperature and low stress led to premature failure of the weld joint in the ICHAZ/FGHAZ. The crack or failure in the weld joint is classified according to the crack location across the joint. The failure classifications are Type I (crack occurs within the weld metal), Type II (crack occurs across the weld metal and HAZ), Type III (crack occurs in the CGHAZ) and Type IV (crack occurs in the FGHAZ or ICHAZ). The Type IV cracking is recognized as the main concern in ferritic steels weld joints under service conditions [10-14].

In the present investigation, creep rupture behaviour of ASME grade 92 steel weld joint and different constituents of heat affected zone (HAZ) of the weld joint have been studied and metallographic investigation have been carried out to have insight of the failure mechanism.

2. Experimental Details

Grade 92 ferritic steel plates of 12 mm thickness were received in normalized (1323 K for 30 minutes) and tempered (1053 K for 2 hour) condition. Chemical composition (wt. %) of the steel is given in Table 1. The plates were butt welded using activated TIG welding process [13,15]. The weld pad was post-weld heat-treated (PWHT) at 1033 K for 4 hours and subsequently X-ray radiographed for its soundness. Different constituents of HAZ of the weld joint microstructures were simulated using isothermal heat treatments. Steel blanks size of 120 mm X 12 mm X 12 mm have been heated to 1448 K, 1203 K, 1133 K for 5 minutes then oil quenched in order to simulate CGHAZ, FGHAZ, ICHAZ respectively. The blanks were PWHT at 1053 K for 2 hours. Creep specimens having dimensions of 5 mm gauge diameter and 50 mm gauge length were fabricated from the joint and HAZs. Tensile test has been carried out on the simulated HAZ constituents at 300 K and 923 K at a strain rate of 3×10^{-3} s^{-1}. Constant load creep tests in air have been carried out at 923 K in the stress range of 150 to 80 MPa on both the weld joint and different constituents of the HAZ. Temperature was controlled within ± 2 K along the gauge length of the specimen during tests. Hardness profiles across the weld joint and different constituents were measured (300 gm applied load and 15 seconds dwell time) by Vickers microhardness. Optical, scanning electron microscope (SEM) and transmission electron microscopic studies were carried out on the different constituents of the joint and simulated constituents of HAZ. Immersion etching for 15 seconds using Villella's reagent (picric acid 5 gm, HCl acid 25 ml, Ethyl alcohol 500 ml) has been employed to reveal the microstructures.

Table 1 Chemical composition (wt. %) of P92 steel base and weld metal.

Elements	**C**	**Cr**	**W**	**Mo**	**Mn**	**Si**	**V**	**N**	**Nb**
P92 Base metal	0.10	9.2	1.9	0.51	0.36	0.27	0.22	0.05	0.07
P92 Weld metal	0.11	9.2	1.9	0.63	0.36	0.28	0.20	0.05	0.07
Elements	**S**	**P**	**Ni**	**Al**	**B**	**Ti**	**N/Al**	**Fe**	
P92 Base metal	0.002	0.01	0.06	0.01	0.001	0.002	5	Bal	
P92 Weld metal	0.002	0.01	0.05	0.01	0.001	0.002	5	Bal	

3. Results and Discussion

3.1 Microstructure and Hardness

Microstructure of the grade 92 steel base metal in the normalized and tempered condition is shown in Fig.1. The steel consists of tempered martensitic lath structure and $M_{23}C_6$ precipitates in the grain and subgrain boundaries and MX precipitates in the intra lath regions. Tungsten content in $M_{23}C_6$ precipitate about 8-12 wt. % has been observed. The precipitates were identified by energy dispersive spectroscopy (EDS) (Fig.1(b)). The microstructures across the HAZ of the joint and simulated HAZs of the joint have been shown in Fig. 2. The grain size of the CGHAZ, FGHAZ and ICHAZ were 25 µm, 11 µm and 6 µm respectively. The simulated grain size of the HAZ microstructural constituents was comparable to the weld joint HAZ constituents at particular temperature region of the weld thermal cycle. The similar grain size variation has been reported in the modified 9Cr-1Mo steel [16]. The hardness variations across the weld joint and simulated constituents of the HAZs were shown in Fig.3. The hardness of the simulated microstructural constituents of HAZ was comparable with the different HAZ constituents hardness across the weld joint. The decrease in grain size and hardness has been observed from simulated coarse grain HAZ (290 VHN) to the intercritical region (204 VHN) of the HAZ and weld joint. A hardness trough was observed in the intercritical region of HAZ of the weld joint. The decrease in hardness in the intercritical region of the HAZ were due to the coarsening of the $M_{23}C_6$ precipitate and sub-grain formation with lower dislocation density [12,13]. The yield stress of the base metal, and simulated CGHAZ, FGHAZ and ICHAZ were 372 MPa, 308 MPa, 240 MPa, 238 MPa respectively at 923 K. The ultimate tensile strength of the base metal, and simulated CGHAZ, FGHAZ and ICHAZ were 384 MPa, 319 MPa, 262 MPa, 246 MPa respectively. It is significant to note that the strength of the ICHAZ and FGHAZ were lower than the base metal and CGHAZ, where hardness measurements shown the similar behaviour.

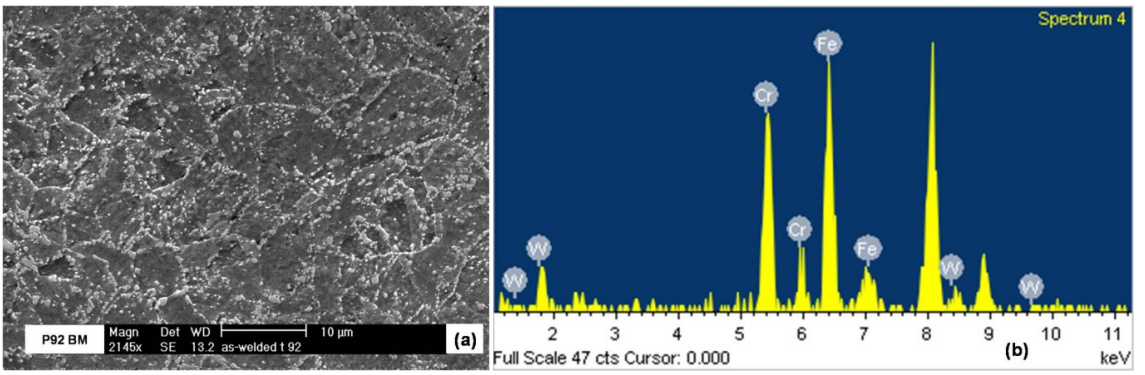

Fig.1. SEM micrograph of P92 steel base metal in the normalized and tempered condition and EDS spectrum of $M_{23}C_6$ precipitate (containing tungsten about 8 wt.%).

3.2 Creep Deformation and Rupture Behaviour of Weld Joint and HAZs

The creep curves of grade 92 steel weld joint and simulated HAZs of the joint at 923 K are shown in Fig.4. The creep curves exhibited primary creep regime followed by an apparent steady state creep deformation and an accelerating tertiary creep regime as in base metal. The variations of creep rate with creep exposure for different constituents of the HAZs are compared in Fig.4. The creep rate decreased with creep exposure to a minimum value

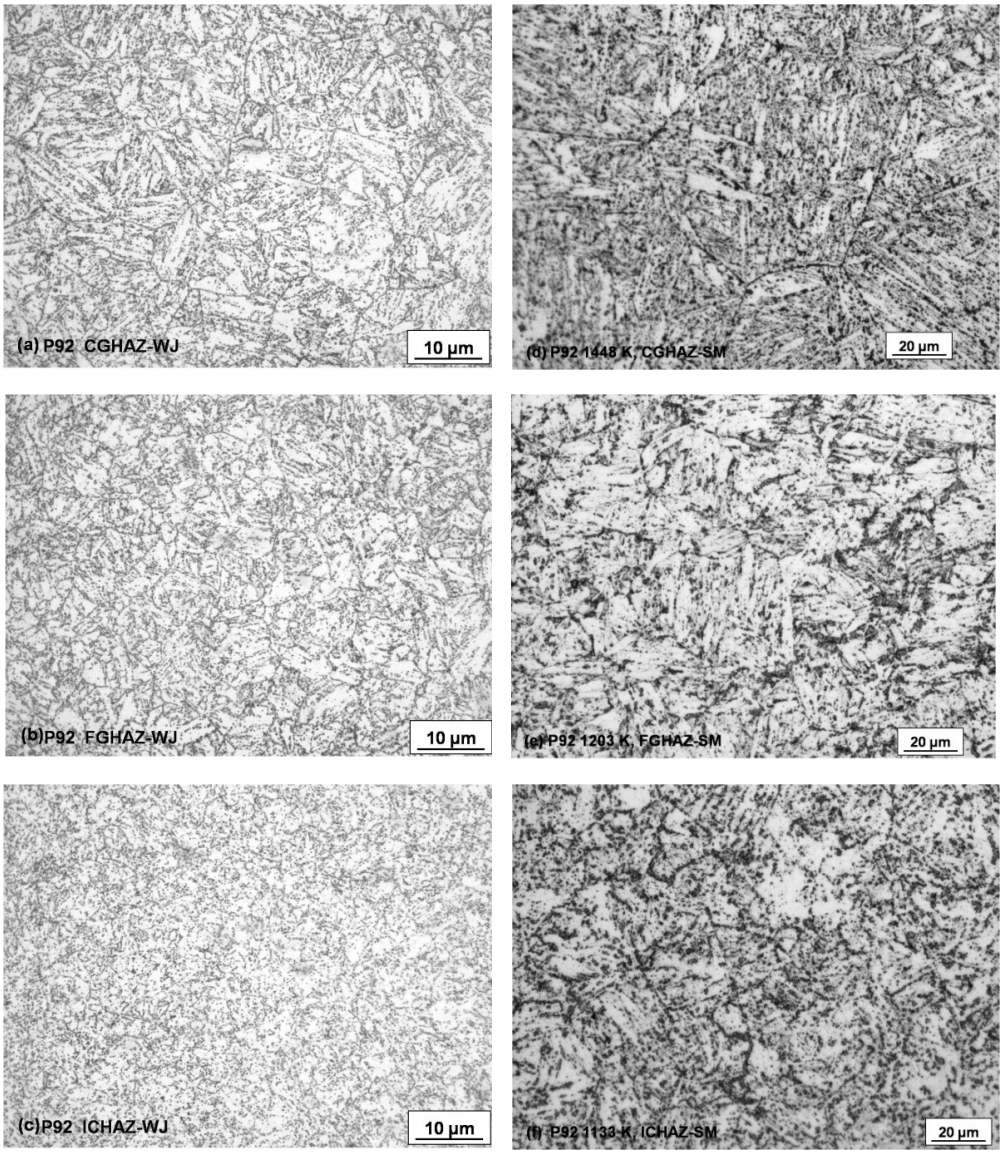

Fig. 2. Variations of microstructures across the HAZ of weld joint of P92 ferritic steel (a) CG-HAZ, (b) FG-HAZ, (c) IC-HAZ and simulated (d) CG-HAZ, (e) FG-HAZ, (f) IC-HAZ.

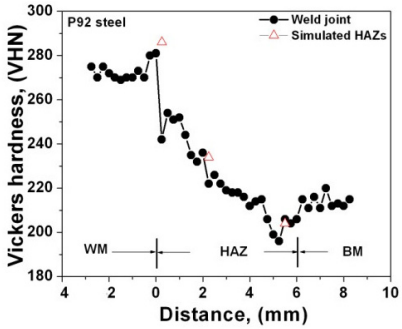

Fig. 3. Variations of hardness across the weld joint and simulated HAZs (CG, FG, IC) of P92 ferritic steel.

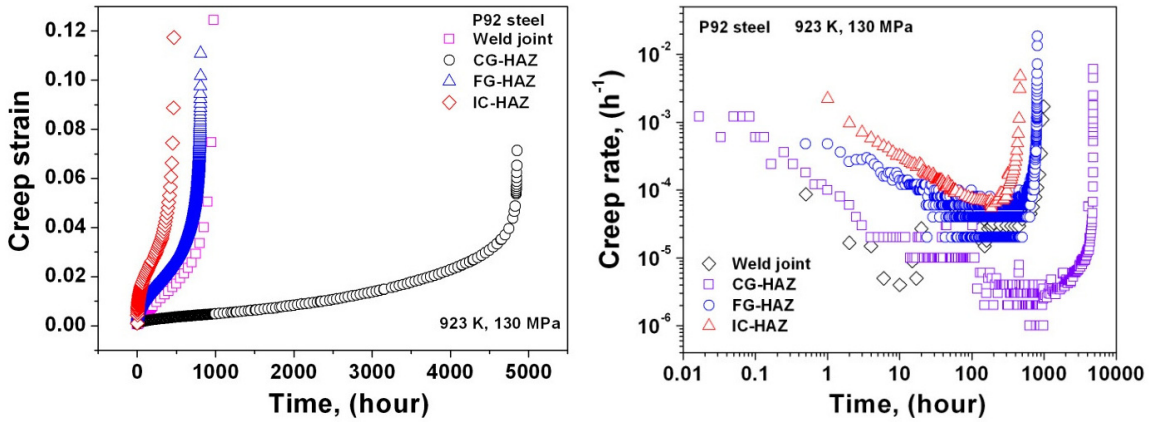

Fig. 4. Creep curves of simulated microstructures of HAZ of the P92 steel joint at 923 K.

followed by increase with no substantial secondary stage of creep deformation. Similar behaviour of creep deformation in tempered martensite ferritic steels has been reported by several investigators [2,5,6,12]. The weld joint exhibited comparable minimum creep rate as in the simulated FGHAZ and ICHAZ. The tertiary stage of creep deformation was found to initiate much early in the ICHAZ of the joint than the weld joint. In normalized and tempered 9Cr-martensitic steel, the occurrence of transient creep has been reported to be the consequence of movement and annihilation of high dislocation density that are introduced in the material during martensitic transformation on normalization heat treatment as well as coarsening of martensite sub-structure and precipitates [4,5,12]. The microstructural instability of the tempered martensite steels with creep exposure is considered for the absence of steady state creep deformation regime [4,5,12].

The variations of rupture life with applied stress for the base, weld joint and simulated HAZ of the joint at 923 K are shown in Fig.5. In both the base metal and weld joint, the variation of creep rupture life with stress showed two-slope behaviour. Rupture lives of the base metal and weld joint were comparable for applied stresses up to around 120 MPa. The weld joint had significantly lower creep rupture life than the base metal for applied stresses lower than around 120 MPa. Difference between the rupture life of weld joint and base metal increased with decrease in applied stress. The early onset of tertiary stage of creep deformation reduced creep rupture life of the weld joint than the base metal. The rupture life of the simulated constituents of HAZs has displayed the significant difference among them. The rupture life of the simulated FGHAZ and ICHAZ were significantly lower than the simulated CGHAZ of the joint and was comparable to the rupture life of the weld joint (Fig.5). Extensive microstructural changes and creep cavitation in selected constituents of the joint have been considered for the early onset of tertiary stage of creep deformation in the steel weld joint. Creep failure location in the weld joint was found to change with applied stress. At stresses higher than around 120 MPa, fracture took place in base metal of the weld joint (Fig.5), whereas at stresses less than 120 MPa failure occurred at the outer edge of HAZ (Fig.5). Failure in the ferritic steel welded joint at the outer edge of HAZ under creep condition is commonly termed as type IV cracking [10,12]. Hardness and metallographic investigation of the creep exposed joint revealed that creep failure of the joint under relatively lower applied stress occurred in the FGHAZ, even though the ICHAZ has lower hardness (Fig.3).

The rupture ductility (reduction in area percentage) of the joint is shown in Fig.5. The shift in failure location from base metal to FGHAZ with increase in rupture life (decrease in applied stress) was accompanied with the drastic reduction in rupture ductility. Similar, low ductility failure has been reported on P92 steel weld joint at applied stresses of 120 MPa and below at 923 K by Wang Xue et al., [17].

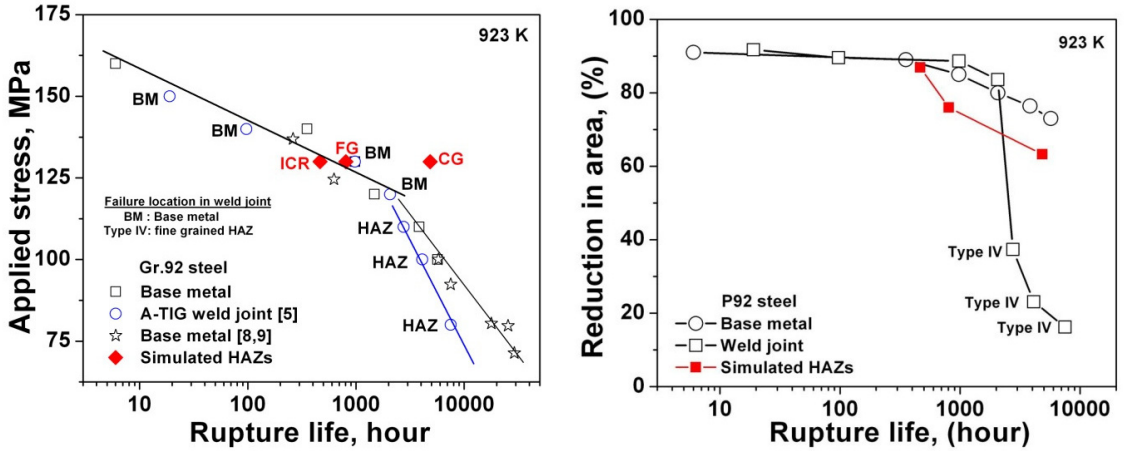

Fig.5. Variations of (a) rupture life with applied stress and (b) reduction in area (%) with rupture life for base metal, weld joint and simulated HAZs of P92 steel at 923 K.

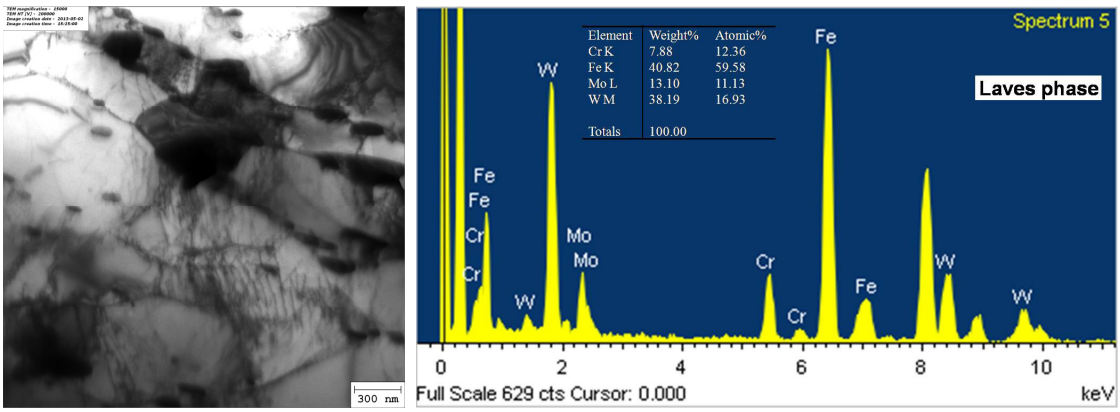

Fig.6. TEM micrographs of creep ruptured FGHAZ of P92 steel weld joint showing extensive Laves phase precipitation at 923 K and 100 MPa.

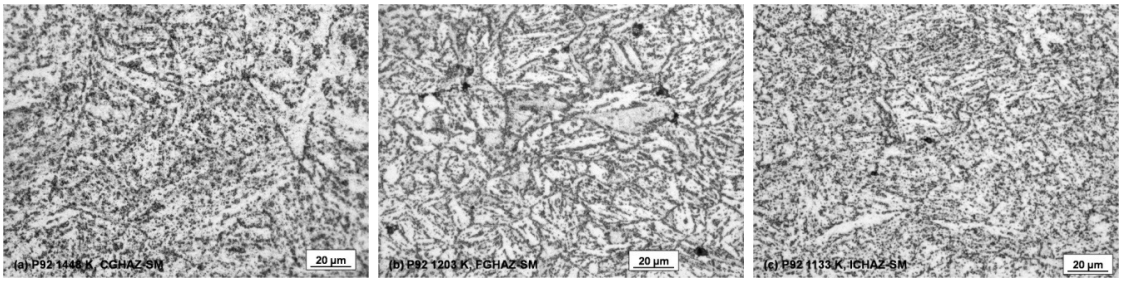

Fig. 7. Variations of creep cavities in the siumulated microstructures HAZ of P92 ferritic steel at 923 K and 130 MPa, (a) CGHAZ, (b) FGHAZ, (c) ICHAZ.

In the present study, the failure in the FGHAZ at 923 K has been observed for applied stresses of 110 MPa and below. The reduction in area (%) of the simulated zones was shown in Fig. 5. The weld joint, base metal and simulated ICHAZ, FGHAZ were comparable.

3.3 Microstructure and Type IV Cracking of the Steel Weld Joint

Microstructure investigation across the creep exposed weld joint revealed that the precipitation of Laves phase across the joint. The precipitate was identified as Fe_2W and was relatively extensive in the FGHAZ in the weld joint (Fig.6). The Laves phase formation across the joint in the grain and subgrain boundaries at the expense of tungsten in solid solution in the matrix was found to predominant under creep condition. The Laves phase size was higher in FGHAZ than the adjacent region of the weld joint under low stress regime. Laves phase size in the present investigation was comparable with the Valeriy Dudko et al., investigations [4]. These observations were evident in comparison with fracture location of the weld joint in the FGHAZ. The creep cavities were found to be associated with Laves phase. This occurs due to the constraint imposed on the particle-soft matrix (due to loss of tungsten in the matrix) interface during creep deformation. The creep cavitation was extensive in the FGHAZ of the joint in the longer duration creep, where fractured occurred in the weld joint. Similarly, the investigation on simulated HAZs shown that the extensive creep cavitation occurred in the FGHAZ than the ICHAZ and CGHAZ (Fig. 7) at 130 MPa stress. The size of the cavities were higher (12 µm) in the simulated FGHAZ than the cavity size 5 µm observed in the (FGHAZ) weld joint. However, longer duration test is planned to assess its integrity of the joint. Hence, reduction in creep strength of the Type IV cracking region under low stress regime has been attributed to the precipitation Laves phase, recovery of lath structures and fine grain size. Variation of hardness across the weld joint on creep exposed specimens is shown in Fig.8. The decrease in hardness with increase in creep exposure period has been observed across the weld joint due to the Laves phase formation, which decreased the strengthening contribution by tungsten in the matrix. The localized creep deformation and cavitation have been found to cause premature Type IV failure of the components associated with weld joint under low stress and at higher temperature [10,12].

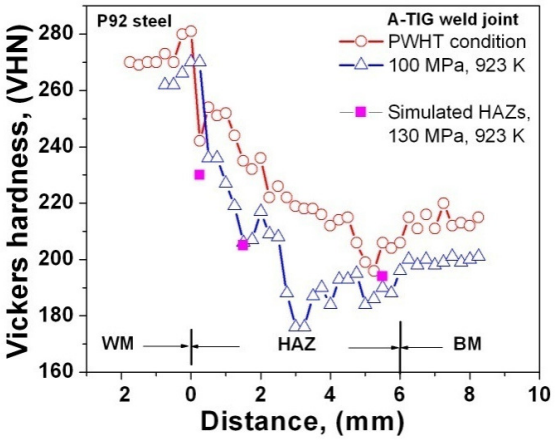

Fig.8.Variation of hardness with distance across the weld joint and simulated HAZs of the joint of P92 steel at 923 K.

4. Conclusions

Creep rupture behaviour of grade 92 steel base metal, weld joint and simulated HAZs were studied at 923 K. Creep rupture life of the base metal and weld joint were comparable under high stress level, whereas lower rupture life with decreased rupture ductility has been observed in the weld joint in comparison with base metal under low stress level. Laves phase formation has been increased with increase in creep exposure and it was extensive in the FGHAZ than the adjacent regions of the weld joint. ICHAZ/FGHAZ shown lower tensile strength and rupture life than the CGHAZ and base metal. Extensive creep cavitation has been observed in the simulated FGHAZ and in the FGHAZ of the joint. Localized creep deformation and cavitation in the FGHAZ under low stress regime led to premature Type IV failure of the weld joint.

Acknowledgements

The authors wish to thank Dr. P.R. Vasudeva Rao, Director, Indira Gandhi Centre for Atomic Research, Dr. T. Jayakumar, Director, Metallurgy and Materials Group and Dr. A.K. Bhaduri, Associate Director, Materials Development and Technology Group, for their keen interest in the work and encouragement.

References

[1]. Ennis P J, Zielinska-Lipiec A, Wachter O, Czyrska-Filemonowicz A, Acta Materialia, Vol. 45, No. 12 (1997), pp. 4901-4907.
[2]. Maruyama K, Sawada K, Koike J, Iron Steel Institute Japan International, Vol. 41, No. 6, (2001), pp. 641–653.
[3]. V´yrostkov´a A, Homolov´a V, Pecha J, Svoboda M, Materials Science and Engineering A 480 (2008) 289–298.
[4]. Valeriy Dudko, Andrey Belyakov, Dmitri Molodov, Rustam Kaibyshev, Metallurgical and Materials Transactions A, Volume 44A (2013) S162-172.
[5]. Irina Fedorova, Alla Kipelova, Andrey Belyakov, Rustam Kaibyshev, Metallurgical and Materials Transactions A, Volume 44A (2013) S128-135.
[6]. Fujio Abe, Materials Science and Engineering A319–321 (2001) 770–773.
[7]. Sawada K, Kubo K, Abe F, Materials Science and Engineering A319-321 (2001) 784-787.
[8]. Jae Seung Lee, Hassan Ghassemi Armaki, Kouichi Maruyama, Taro Muraki, Hitoshi Asahi, Materials Science and Engineering A 428 (2006) 270–275.
[9]. Fujimitsu Masuyama, International Journal of Pressure Vessels and Piping, 87 (2010) 617-623.
[10]. Sawada K, Hongo H, Watanabe T, Tabuchi M, Materials Characterization 61 (2010) 1097-1102.
[11]. Yin Zhong Shen, Sung Ho Kim, Chang Hee Han, Hai Dong Cho, Woo Seog Ryu, Journal of Nuclear Materials 384 (2009) 48–55.
[12]. Laha K, Chandravathi K S, Parameswaran P, Bhanu Sankara Rao K, Mannan S L, Metallurgical and Materials Transactions A, Volume 38A (2007) 58-68.
[13]. Sakthivel T, Vasudevan M, Laha K, Parameswaran P, Chandravathi K S, Mathew M D, Bhaduri A K, Materials Science and Engineering A 528 (2011) 6971 - 6980.
[14]. Yoshizawa M, Igarashi M, Moriguchi K, Iseda A, Hassan Ghassemi Armaki, Maruyama K, Materials Science and Engineering A 510–511 (2009) 162–168.
[15]. Vasudevan M, Computational and Experimental Studies on Arc Welded Austenitic Stainless Steels, PhD Thesis, 2007, Indian Institute of Technology, Madras, India.
[16]. Chandravathi K S, Laha K, Bhanu Sankara Rao K, Mannan S L, Materials Science and Technology, 2001, Vo.17, 559-565.
[17]. Wang Xue, Pan Qian-gang, Ren Yao-yao, Shang Wei, Zeng Hui-qiang, Liu Hong, Materials Science and Engineering A 552 (2012) 493– 501.